

OPTIMIZED USE OF DIVERSITY MODES IN TRANSMITTER DIVERSITY SYSTEMS

James K. Cavers

School of Engineering Science
Simon Fraser University
8888 University Drive, Burnaby, B.C. V5A 1S6 Canada
e-mail: cavers@sfu.ca

Abstract – This paper examines the optimized allocation of a fixed transmitter power budget among several transmitter diversity paths that are correlated and/or of dissimilar strengths. Under these conditions, algorithms for optimum allocation differ significantly from conventional transmitter diversity and provide better performance. Simplified algorithms with negligible performance loss are also presented.

I. INTRODUCTION

Transmitter diversity can achieve diversity in the downlink, even if the mobile has only a single antenna. The method uses multiple base station antennas and keeps their signals separated by assigning them different CDMA spreading codes (or different delays of the same code) or by using space-time codes [1]-[3]. The performance of such methods has been shown [1] to approach that of receiver diversity at the mobile, the latter being a less desirable configuration for reasons of cost.

This paper examines a neglected optimization in transmitter diversity. It was motivated by three observations. First, not all diversity paths have the same mean square gain. Examples include polarization diversity and macrodiversity. Second, paths are often correlated, as from transmitter antennas without enough separation for full diversity, especially when they transmit to a mobile nearing the end-fire direction of a linear array. Finally, the total transmitter power is a finite resource.

The question examined in the paper is therefore how to allocate transmitter power among the transmitter diversity paths of various strengths and correlations in order to minimize the overall bit error rate. In the interest of brevity, the treatment assumes explicit diversity channels separable by the receiver using different CDMA spreading codes. A more complete treatment that includes the effect of space-time coding to

separate the diversity modes will be presented separately.

II. SYSTEM AND SIGNAL MODELS

Transmitter, Channel and Receiver

Here we outline the simplest model, in which the diversity branches are independent. We extend the model to correlated branches in Section IV, where we generalize from diversity branches to diversity modes. Fig. 1 shows the transmitter using PSK modulation with a different spreading sequence pulse shape $p_i(t)$, $i = 1 \dots L$ on each of L antennas. The branches experience independent Rayleigh fading and are picked up on the receiver's single antenna embedded in white noise $v(t)$. The receiver employs the appropriate despreading matched filter to separate the branch signals, and obtains a noisy sample of the transmitted data r_i , together with an estimate \hat{g}_i of the channel gain obtained by pilot tones, pilot symbols, or similar means.

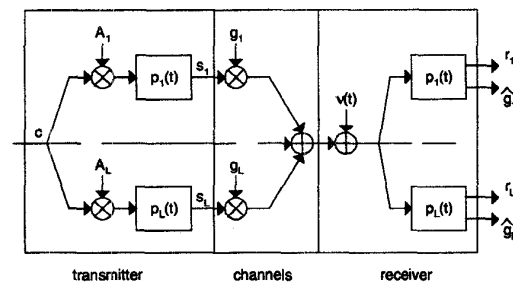


Fig. 1: Basic Transmitter Diversity

The branch- i sample at symbol time k is then

$$r_i(k) = A_i g_i(k) c(k) + n_i(k) \quad (1)$$

where the constellation point $c(k)$ has $E[|c(k)|^2] = 1$, A_i is the amplitude the transmitter applies to channel i , $g_i(k)$ is the complex Gaussian channel gain with variance $\sigma_{g_i}^2 = \frac{1}{2} E[|g_i(k)|^2]$ and $n_i(k)$, the projection of $v(t)$ onto the despreading sequence, is complex white Gaussian noise with $\frac{1}{2} E[|n_i(k)|^2] = N_o$. The channel gains may have different variances.

To distinguish the effects of the average channel gain from the power invested by the transmitter, we represent the SNR per branch as

$$\Gamma_i = \frac{A_i^2 \sigma_{g_i}^2}{N_o} = P_i G_i \quad (2)$$

where G_i is the SNR that would be experienced with unit transmitted power, representing the attenuation of channel i , and P_i is the transmitter power relative to one watt. Both P_i and G_i are therefore dimensionless.

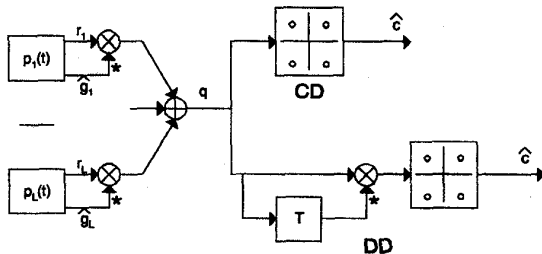


Fig. 2: Detection at the Mobile Receiver

As shown in Fig. 2, the receiver uses the channel estimates, assumed to be perfect in this study, to form a maximal ratio combination (MRC) [4] $q = \sum_{i=1}^L r_i \hat{g}_i^*$ of the several branches. From q , the receiver produces a decision $\hat{c}(k)$ in either of two ways. The natural way (labeled MRC/CD) is coherent detection: simply map q onto the nearest constellation point, and decide the bit identity according to the polarities of its real and/or imaginary parts. An alternative, labeled MRC/DD, is to differentially detect q , then map the result to the constellation. Operationally, this latter method makes little sense, since the combining structure has already exploited what coherence exists in the signals. However, its bit error rate has a simple expression that we can use to gain analytical insight. We restrict our attention to MRC/DD in this paper.

Error Rate With Perfect CSI

With perfect channel state information, the MRC/DD detector has a well-known expression for error rate when the branches fade independently. For BPSK, the error rate [4, eqn. 10-8-3], is

$$P_e = \frac{1}{2} P_e = \frac{1}{2} \prod_{i=1}^L \frac{1}{1 + \Gamma_i} \quad (3)$$

whether the branch SNRs are distinct or equal. As noted in [4], (3) can be interpreted as the product of twice the per-branch error rates. For large SNRs, the expression is asymptotic to the product of branch SNRs

$$P_e \approx \frac{1}{2} \frac{1}{\prod_{i=1}^L \Gamma_i} \quad (4)$$

III. OPTIMIZED PERFORMANCE

Continuous Optimization

Our objective is straightforward: to minimize the error probability (3) with respect to the branch powers P_i , subject to a constraint on the total transmitted power $\sum_{i=1}^L P_i = P_t$ (we also constrain powers to be non-negative). Let us first consider the asymptotic case, in which all SNRs $\Gamma_i \gg 1$. Substituting (2) into (4) and using a Lagrange multiplier η gives the objective function

$$J = \frac{1}{2} \frac{1}{\prod_{i=1}^L P_i G_i} + \eta \left(\sum_{i=1}^L P_i - P_t \right) \quad (5)$$

Setting all $\partial J / \partial P_i = 0$ and making use of (4) gives

$$P_i = \frac{P_e}{2\eta} = \frac{P_t}{L} \quad (6)$$

where the second equality makes use of the constraint. We therefore have the interesting result that all branches with large SNRs should receive the same transmit power, regardless of the branch gains. This is reassuring, because it is the usual method.

Next, consider the more general case (3), which gives the objective function

$$J = \frac{1}{2} \prod_{i=1}^L \frac{1}{1 + P_i G_i} + \eta \left(\sum_{i=1}^L P_i - P_t \right) \quad (7)$$

Differentiating with respect to each of the powers P_i and making use of (3) gives

$$P_i = \max\left(\frac{P_e}{\eta} - \frac{1}{G_i}, 0\right) \quad (8)$$

Equating the sum of the branch powers to P_t allows solution for P_e/η , and substituting that value back into (8) gives the optimum powers in terms of the unit-power noise-to-signal (NSR) ratios G_i^{-1} as

$$P_i = \frac{P_t}{L} + \frac{1}{L} \sum_{k=1}^L G_k^{-1} - G_i^{-1} \quad (9)$$

provided the branch powers (8) are greater than zero.

Some care is required in interpreting (9). For example, the asymptotic equipower allocation (6) is evident for large enough total power P_t . However, the sum of the second and third terms is negative for any branch with NSR less than the average. Consequently, the weakest branch will cut out as the transmitter power P_t decreases, leaving that power to be spread among the stronger branches. Assume that the branches are sorted in order of decreasing G_i . Then the easiest calculation for the set of branch powers evaluates (9) for $i=L$; if it is not positive, then P_L is set to zero and L is reduced by one; and we repeat for $i=L-1$, $i=L-2$, ..., $i=1$. The behaviour is shown in Fig. 3 for $L=3$ and unit-power SNRs $G_1=1$, $G_2=0.2$ and $G_3=0.05$, along with the equipower curve.

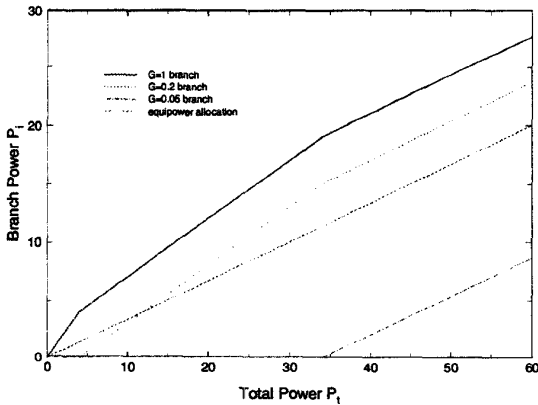


Fig. 3: Optimum Power Allocation

Next, we examine the effect of the optimization on error performance. We define two "test sets" on which to compare algorithms: a three-branch set with

$$G_1 = 1, G_2 = 0.05, G_3 = 0.01 \quad (10)$$

and a two-branch set with

$$G_1 = 1, G_2 = 0.01 \quad (11)$$

That is, the gains of the weak branches are 13 dB or 20 dB below that of the main branch.

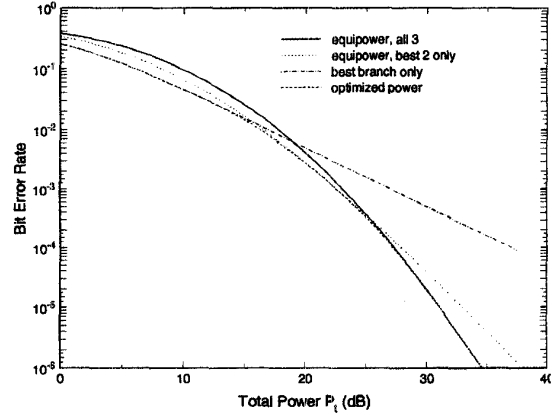


Fig. 4: Performance Comparison, $L=3$

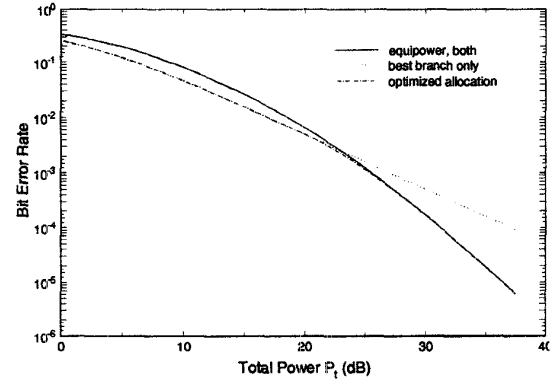


Fig. 5: Performance Comparison, $L=2$

Fig. 4, for the $L=3$ test set (10), compares the performance of an optimized power system against systems that everywhere split the power equally among: all the branches; the best two; and the best one. Fig. 5 is its counterpart for the $L=2$ test set (11). In both graphs, the optimized system rides just under the infimum of the other curves. We make two observations. First, at high SNR, the weak branches provide a significant diversity SNR benefit, and are worth using, even though their path gains are 13 dB and 20 dB below that of the strongest branch. Second, at low SNR, the weak branches simply waste power, and should not be used. The optimized power system transitions smoothly between these regimes.

Switched Optimization

The optimized power system tracks the equipower systems quite closely if we account for the varying number of branches used. This suggests a simpler system in which branches are used either with an equipower allocation or not at all. That is, a set of thresholds on P_i determines where to add or drop a branch, and the total power is split equally among the current set of branches. To calculate the threshold T_l between l branches and $l+1$, equate the two error rates with total power diluted among the appropriate number of branches. From (3) we have

$$\prod_{i=1}^l \left(1 + \frac{T_l}{l} G_i\right) = \prod_{i=1}^{l+1} \left(1 + \frac{T_l}{l+1} G_i\right) \quad (12)$$

which we solve numerically for threshold T_l . The performance of such a system is shown in Fig. 6 for both test sets. It is graphically coincident with that of the optimized power systems shown in Figs. 4 and 5 and reproduced in Fig. 6. We conclude that it is sufficient to operate a system with transmitter power divided equally among those branches that are strong enough to be used.

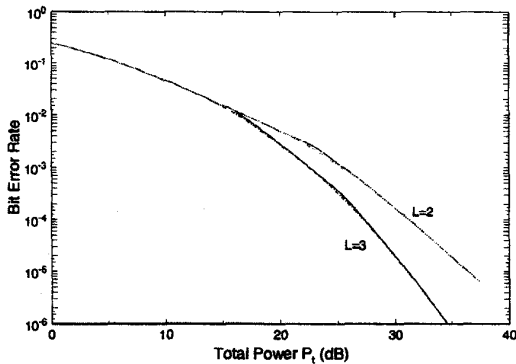


Fig. 6: Simple Switched, Optimum Switched and Continuously Optimum Strategies.

A simpler and more illuminating strategy stems from calculation of the SNR of the weakest branch at the threshold where it is dropped. Table 1 presents the SNR values $\Gamma_l = T_{l-1} G_l / l$ of branch l at its threshold T_{l-1} for the two configurations (10) and (11).

	T_1	T_2
L=3	0.95	1.13
L=2	0.99	N/A

Table 1: Weak Branch SNRs at Their Drop Point

The Table shows that the weakest branch SNRs at the add/drop point are approximately unity. The simplified switching strategy therefore replaces the optimum threshold criterion (12) with $T_l = (l+1)/G_{l+1}$, the value of P_i that makes the SNR of branch $l+1$ equal to unity. Its performance is also shown on Fig. 6, with the continuously optimum power curve of the previous section for comparison. Clearly, the simplified and the optimum strategies give almost identical performance.

IV. CORRELATED BRANCHES

To this point, we have dealt only with independent branches of various strengths. Of equal interest, however, is correlation among the branch gains g_i . It results in a smaller diversity improvement than if they fade independently. The question at hand is how to optimize use of the diversity that remains.

To begin, we generalize from diversity branch (i.e., an antenna) to diversity mode. Pack the branch gains into a length- L vector \mathbf{g} with covariance matrix \mathbf{R}_g . The unitary matrix \mathbf{X} of eigenvectors of \mathbf{R}_g produces a decorrelated set of gains \mathbf{g}' by means of the change of variables $\mathbf{g}' = \mathbf{X}^H \mathbf{g}$, giving a diagonal covariance matrix

$$\mathbf{R}'_g = \Lambda \quad (13)$$

where $\Lambda = \text{diag}(\lambda_1, \dots, \lambda_L)$ is the matrix of eigenvalues of \mathbf{R}_g . These diversity modes, summarized by the columns of \mathbf{X} , are independent and have different mean-square strengths given by $\lambda_1, \dots, \lambda_L$, analogous to $\sigma_1^2, \dots, \sigma_L^2$ when the branches fade independently. If we can excite the modes individually, we will have reproduced the model used in Sections II and III, the results of which can then be applied directly to the case of correlated branches.

To keep the modes separate, we now associate a different spreading sequence $p'_k(t)$, $k=1, \dots, L$ with each mode, rather than with each branch, and use amplitude A_{ki} as the amplitude given to mode k on branch i . Thus the signal transmitted on antenna i is

$$s_i(t) = c \sum_{k=1}^L A_{k,i} p'_k(t) \quad (14)$$

The receiver picks up the single signal $\sum_{i=1}^L g_i s_i(t) + \nu(t)$ and separates the modes by despreading with their sequences to produce r'_1, \dots, r'_L .

We pack these samples into a column vector \mathbf{r}' , and note that it equals

$$\mathbf{r}' = c\mathbf{A}\mathbf{g} + \mathbf{n}' \quad (15)$$

where the (k,i) component of \mathbf{A} is $A_{k,i}$ and \mathbf{n}' is the projection of $\nu(t)$ onto the despreading sequences. We structure \mathbf{A} as

$$\mathbf{A} = \mathbf{A}'\mathbf{X}^H \quad (16)$$

where $\mathbf{A}' = \text{diag}(A'_1, \dots, A'_L)$ contains the amplitudes given to the modes (Fig. 7).

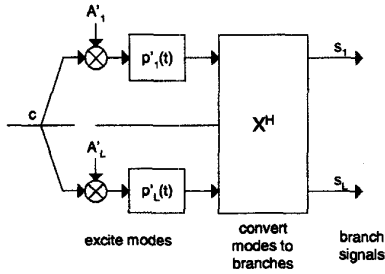


Fig. 7: Separate Excitation of Diversity Modes

Substitution of (16) into (15) yields

$$\mathbf{r}' = c\mathbf{A}'\mathbf{g}' + \mathbf{n}' \quad (17)$$

Row k of (17) is $r'_k = A'_k g'_k + n'_k$, which demonstrates that we have separately excited the independent diversity modes.

As for the power invested by the system, the power transmitted on antenna i is just $\sum_{k=1}^L A_{k,i}^2$ since the spreading codes are orthogonal or approximately so. Consequently, the total power is

$$P_t = \text{tr}[\mathbf{A}\mathbf{A}^H] = \sum_{k=1}^L A_k'^2 = \sum_{k=1}^L P_k' \quad (18)$$

where the second equality follows from substitution of (16).

From (17) and (18), we see that our decorrelated problem is now identical to the one analyzed in Sections II and III - independently fading branches of various mean square gains - and all those results apply equally to decorrelated fading. We can create test sets by assuming branch gains with equal mean square value, intercorrelated so that: for $L=3$, adjacent antenna pairs have a correlation coefficient of 0.94 and the first and third antennas have a correlation coefficient of 0.86; and for $L=2$, the antennas have a correlation coefficient of 0.98. These values were selected so that the eigenvalues of the modes are in the same ratios as (10) and (11). All the results of Figs. 4 to 6 therefore apply directly to these

correlated branch test sets and so do the control algorithms; for example, as P_t decreases, we cease to excite the weakest diversity mode, then the second weakest, and so on.

This optimum strategy differs significantly from conventional transmitter diversity. In the latter scheme, we would assign equal amplitude A , but a different spreading code, to each branch. After despreading by the receiver, the vector of branch components would be $\mathbf{r} = c\mathbf{A}\mathbf{g} + \mathbf{n}$, which could then be decorrelated to

$$\mathbf{r}' = \mathbf{X}^H \mathbf{r} = c\mathbf{A}'\mathbf{g}' + \mathbf{n}' \quad (19)$$

For high SNR, this assigns equal transmit power to each mode, as in the optimized allocation. However, it does not abandon modes as the transmit power decreases, making its performance equivalent to the equipower, all branch, curves in Figs. 4 and 5. It therefore has poorer performance than the optimized system at lower SNRs. To contrast the two approaches, consider a pair of tightly correlated diversity branches. Conventional transmitter diversity would keep different spreading sequences and equal power on each branch, regardless of transmit power, whereas optimized diversity below a threshold level would drop the weak mode and use the *same* spreading sequence on each branch.

V. CONCLUSIONS

We have optimized transmitter diversity for the case of diversity branches with differing mean square strengths, or correlated gains, or both. Optimum here means minimum error rate for a given investment in transmitter power. A power allocation algorithm that is almost as good as the optimum is simply to give all diversity branches the same power, except for those with branch SNR less than unity, which are removed and the power reallocated to stronger branches. Performance curves show that even branches that are 20 dB weaker than the main branch contribute significant diversity improvement at high SNR; conversely, they are a drain on the system at low SNR.

When branches are correlated, we work in terms of decorrelated modes, and give each mode, rather than each branch, its own spreading code and power allocation. Even if a pair of equipower branches is highly correlated, with a correlation coefficient of 0.98, there is valuable diversity to be gained at high SNR. This optimized transmitter diversity algorithm differs significantly from conventional transmitter diversity, particularly as the weak modes are dropped.

When branches are uncorrelated and of equal power, optimization results in the conventional solution of equipower operation.

REFERENCES

- [1] J.H. Winters, "The Diversity Gain of Transmit Diversity in Wireless Systems with Rayleigh Fading", *IEEE Trans Veh Technol*, vol 47, no 1, pp 119-123, February 1998.
- [2] J.-C. Guey, M.P. Fitz, M.R. Bell and W.-Y. Kuo, "Signal Design for Transmitter Diversity Wireless Communication Systems over Rayleigh Fading Channels", *IEEE Veh Technol Conf*, pp. 136-140, Atlanta, 1996.
- [3] V. Tarokh, N. Seshadri and A.R. Calderbank, "Space-Time Codes for High Data Rate Wireless Communication: Performance Analysis and Code Construction", *IEEE Trans Inf Th*, March 1998.
- [4] M. Schwartz, W. Bennett and S. Stein, *Communication Systems and Techniques*, McGraw-Hill, 1966.